patients. Thus, the facial artery can be used as an important landmark in the course of the nerve. The pulsations of the facial artery can be readily palpated by the surgeon at the anteroinferior angle of the masseter muscle. This landmark is an important guide in locating the marginal mandibular nerve during surgical procedures.[6]

But, once these anatomical structures or landmarks are changed, it will increase the difficulty of surgery and the possibility of nerve damage. In this study, facial nerve monitoring led to successful localization and dissection of the MMB. Nerve stimulation and evoked electromyography are becoming increasingly accepted in various fields of surgery for nerve identification and preservation. According to Lowry et al,[7] the most common reasons for using intraoperative monitoring were as follows: to help identify the nerve (20%), medicolegal concerns (14%), increased safety (11%), and the belief that FNM was standard of care (11%).

Intraoperative nerve monitoring is a common technology in modern surgery. We try to draw the attention that mandibular tumor surgery may also lead to facial nerve injuries, especially giant tumor resection. Some researchers try to find a precise method of preoperative percutaneous facial nerve mapping to avoid from accidental injury.[8] Maybe, it will play a greater role in future works. We emphasize 2 advantages of facial nerve monitoring during surgery of giant mandibular tumor. First, tumor volume increase will result in the change of nerve anatomy, by preoperatively using a nerve stimulator with a probe having to identify the MMB location when the mandibular landmarks have changed, the location of MMB becomes much easier, thereby saving operative time. Second, the most common pattern of MMB was nerve with 2 branches,[9] when the mandibular tumor becomes larger, nerve dissection should be longer, and the more likely damage to the small branch of MMB branches, which also lead to a final weakness and cosmetic deformity of mouth, the branches can be reliably identified with this method.

CONCLUSIONS

We achieved successful intraoperative MMB preservation by using a nerve stimulator in the giant mandibular tumor surgery. We conclude that if landmarks of mandible have changed, facial nerve monitoring may assist in avoiding accidental nerve injury. We recommend this method because of its simplicity, reliability, and effectiveness. Last, much attention should be paid to MMB of facial nerve during mandible surgery, especially in giant tumor resection.

REFERENCES

1. Romanes GJ. Cunningham's Textbook of Anatomy. 12th ed. Oxford, UK: Medical Publications; 1987:756–759
2. Stern SJ. Precise localization of the marginal mandibular nerve during neck dissection. *Head Neck* 1992;14:328–331
3. Krauze F. Surgery of the Brain and Spinal Cord: Based on Personal Experiences Nabu Press; 2013
4. Minahan RE, Mandir AS. Neurophysiologic intraoperative monitoring of trigeminal and facial nerves. *J Clin Neurophysiol* 2011;28:551–565
5. Bron LP, O'Brien CJ. Facial nerve function after parotidectomy. *Arch Otolaryngol Head Neck Surg* 1997;123:1091–1096
6. Batra AP, Mahajan A, Gupta K. Marginal mandibular branch of the facial nerve: an anatomical study. *Indian J Plast Surg* 2010;43:60–64
7. Lowry TR, Gal TJ, Brennan JA. Patterns of use of facial nerve monitoring during parotid gland surgery. *Otolaryngol Head Neck Surg* 2005;133: 313–318 Erratum in: *Otolaryngol Head Neck Surg*. 2005;133:1000
8. Lin B, Lu X, Shan X, et al. Preoperative percutaneous nerve mapping of the mandibular marginal branch of the facial nerve. *J Craniofac Surg* 2015;26:411–414
9. Karapinar U, Kilic C, Cetin B, et al. The course of the marginal mandibular branch of the facial nerve in adult cadavers. An anatomic study. *Saudi Med J* 2013;34:364–368

OPEN

Influence of Orbital Implant Length and Diameter on Stress Distribution: A Finite Element Analysis

Zhang Xing, DMD, Ling Song Chen, DMD,† Wei Peng, DMD,† and Ling Jian Chen, MD**

Purpose: A mathematical simulation of stress distribution around orbital implants was used to determine which length and diameter of implants would be best to dissipate stress.

Methods: An integrated system for computed tomography data was utilized to create a 3-dimensional model of craniofacial structures. The model simulated implants placed in the 7, 11, and 12 o'clock positions of the orbital rim. A load of 2 N was applied to the model along the long axis of the implant (model 1) and an angle of 45° with the long axis of the implant (model 2). A model simulating an implant with a diameter of 3.75 mm and lengths of 3, 4, 6, 8, and 10 mm was developed to investigate the influence of the length factor. The influence of different diameters was modeled using implants with a length of 6 mm and diameters of 3.0, 3.75, 4.2, 5.0, and 6.0 mm. Values of von Mises equivalent stress at the implant–bone interface were computed using the finite element analysis for all variations.

Results: The elements exposed to the maximum stress were located around the root of the orbital implant in model 1 or between the neck and the first thread of the orbital implant in model 2. An increase in the orbital implant diameter led to a decrease in the maximum von Mises equivalent stress values. In model 1, the reductions were 45.2% (diameter of 3.0–3.75 mm), 25.3% (diameter of 3.75–4.2 mm), 17.2% (diameter of 4.2–5.0 mm), and 5.4% (diameter of 5.0–6.0 mm). In model 2, the reductions of the maximum stress

From the *Department of Stomatology, Guangdong Provincial Hospital of Traditional Chinese Medicine; and †Department of Oral and Maxillofacial Surgery, First Affiliated Hospital, Sun Yat-sen University, Guangzhou, China.

Received August 7, 2016.
Accepted for publication September 22, 2016.

Address correspondence and reprint requests to Associate Professor Zhang Xing, DMD, Department of Stomatology, Guangdong Provincial Hospital of Traditional Chinese Medicine, Guangzhou, China; E-mail: zhangxing2698@163.com

This study was supported by the Guangdong Province, Science and Technology Institution Foundation (Grant Nos. 2010B060900070, 2011B010200008) and National Natural Science Foundation of China (Grant No. 81371111).

The authors report no conflicts of interest.

ISSN: 1049-2275
DOI: 10.1097/SCS.0000000000003305

values were 51.9%, 35.4%, 19.7%, and 8.1% respectively. However, the influence of orbital implant length was not as pronounced as that of diameter. In model 1, the reductions were 28.8% (length of 3–4 mm), 19.2% (length of 4–6 mm), 9.6% (length of 6–8 mm), and 4.3% (length of 8–10 mm). In model 2, the reductions of the maximum stress values were 35.5%, 21.1%, 10.9%, and 5.4% respectively.

Conclusions: An increase in the implant diameter decreased the maximum von Mises equivalent stress around the orbital implant more than an increase in the implant length. From a biomechanical perspective, the optimum choice was an orbital implant with no less than 4.2 mm diameter allowed by the anatomy.

Key Words: Implant diameter, implant length, orbital implants, stress distribution, three-dimensional finite elemental analysis

Surgical reconstruction of the orbital after tumor resection and exenteration is challenging. Orbital osseointegrated implants can be surgically installed to guarantee secure retention of the prosthesis.[1–4] However, success rate of orbital implants between 35% and 75% after 3 to 14 years observation depends on the sites of insertion and the dimension of the orbital implants.[5–8] Failure takes place after orbital implant loading and is associated primarily with bone loss around the implant neck. Stress distribution created in the bone depends on the dimension of the orbital implants. Clinicians must determine the most appropriate dimensions of orbital implants in developing treatment plans to minimize hazardous stress concentration in the supporting bone.[9,10] However, the influence of the orbital implant length and diameter on stress distributions in craniofacial bones has not yet been described.

An integrated system for three-dimensional (3D) data utilization in craniofacial applications that allows 3D scanning, solid modeling, and finite element analysis has been developed by the authors. In this study, a digital biomechanical model of the craniofacial skeleton, created from computed tomography (CT) scanning data, was used to analyze the influence of orbital implant diameter and length on stress distribution around the implant.

METHODS

Craniofacial Model Construction

A 3D, finite element, solid model of the human skull was constructed based on CT data.[11] A 24-year-old healthy volunteer without orbital bone deossification was arbitrarily chosen. The craniofacial part of the skull was scanned with a spiral CT scanner at an axial plane (120 kV, 25 mA, 1 mm slice thickness, 1 mm slice distance, voxel size $0.3 \times 0.3 \times 2\,mm^3$) from below the zygomatic bone to 4 cm above of the supraorbital margin. The CT Digital Imaging and Communications in Medicine data were analyzed with 3D scanning software (RapidFormTM, INUS Technology Inc, Seoul, Korea). This generated a polygonal isosurface and shell and fit nonuniform rational Bspline surfaces. Three-dimensional reconstructions of these parts were edited and optimized polygonal surfaces were exported to the downstream application. The orbital bone consists of both trabecular and cortical bone, and correct representation of the mechanical properties of these different bone types in finite element models is important for accurate results. The output data were transferred to 3D computer-aided design software (ANSYS Workbench, ANSYS Inc, Canonsburg, PA) for finite element solid model conversion (Fig. 1A).

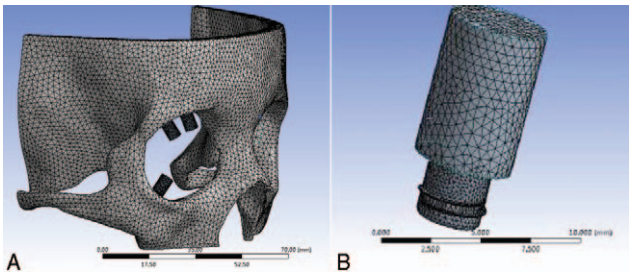

FIGURE 1. Three-dimensional finite elemental meshing model. (A) Craniofacial model. (B) Orbital implant model with length of 3 mm, diameter of 3.75 mm, and an abutment 7 mm in height.

Implant Model Construction

The craniofacial Vistafix System implant (Entific Medical Systems, Göteberg, Sweden) and titanium abutment 7 mm in height were constructed using 3D computer-aided design software. The 3D implant models represented commonly available submerged titanium solid cylinder-shaped craniofacial implant with 0.5 mm thread pitch (Fig. 1B). The implants were placed into the 7, 11, and 12 o'clock positions of the right orbital rim in the vertical position. Implant models with a diameter of 3.75 mm and lengths of 3, 4, 6, 8, 10 mm were used to investigate the influence of length as a factor. The influence of diameter was modeled by implants with a length of 6 mm and diameters of 3.0, 3.75, 4.2, 5.0, and 6.0 mm.

Material Properties and Meshing

All materials used in the models were considered homogeneous, isotropic, and linearly elastic. Poisson ratio (μ) and Young modulus (E) were 0.3 and 14.7 GPa for the cortical bone, 0.3 and 0.49 GPa for the cancellous bone, and 0.33 and 117 GPa for the implants, respectively. All interfaces between the materials were assumed to be bonded or osseointegrated. These models were read into a finite elemental program (COSMOS/Works, Structural Research & Analysis Corp, Los Angeles, CA) for mesh generation. Each model was meshed by elements defined by 8 nodes with 3 degrees of freedom in tetrahedral bodies (Solid 45). Each model consisted of approximately 190,000 elements and 290,000 nodes.

Loading and Boundary Conditions

Usually, the orbital prostheses was fixed by magnetic attachments, the average of force (including the weight of prostheses and magnetic retentive force) was approximately 2 N.[4] Therefore, a load of 2 N was applied to the model along the long axis of the implant (model 1) and an angle of 45° with the long axis of the implant (model 2). With regard to boundary conditions, movement was restricted to the zygomatic bone plane and 4 cm above the supraorbital margin. The von Mises equivalent stress distribution in the orbital bone for each model was calculated by the finite elemental program.

RESULTS

The mathematical analysis demonstrated an uneven stress distribution inside the bony socket around the loaded implants. The elements exposed to the maximum stress were located around the root of the orbital implant in model 1 (Fig. 2A and B) or between the neck and the first thread of the orbital implant in model 2 (Fig. 2C and D).

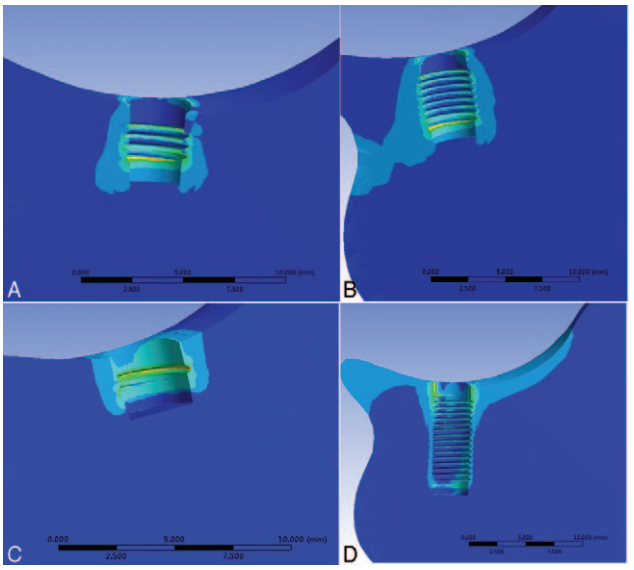

FIGURE 2. Distribution of von Mises equivalent stress around implants with different diameters and lengths. View is from inside bony socket. The maximum stress was located around the root of the orbital implant in model 1 or between the neck and the first thread in model 2. (A) Model computed for implant with diameter of 4.2 mm and length of 6 mm in model 1. (B) Implant with diameter of 3.75 mm and length 3 mm. (C) Implant with diameter of 4 mm and length of 3 mm in model 2. (D) Implant with diameter of 5 mm and length 10 mm in model 2.

These maximum stress locations were identical for all implant lengths and diameters.

A comparison with maximum stress for implants of the same length but different diameters showed distinct variances. The plotting of maximum stress for implant diameters, varying from 3.0 to 6.0 mm, indicates a marked influence of the implant diameter on stress in the orbital bone (Fig. 3A and B). In model 1, the maximum stress value in the bone around the orbital implant with a diameter of 3.75 mm was 45.2% smaller than the diameter of 3.0 mm implant. Stress reduction continued to decrease for larger diameters. The reductions of the maximum stress values were 25.3% (diameter of 3.75–4.2 mm), 17.2% (diameter of 4.2–5.0 mm), and 5.4% (diameter of 5.0–6.0 mm), respectively. In model 2, the reductions of the maximum stress values in the bone around the orbital implant were 51.9% (diameter of 3.0–3.75 mm), 35.4% (diameter of 3.75–4.2 mm), 19.7% (diameter of 4.2–5.0 mm), and 8.1% (diameter of 5.0–6.0 mm) respectively.

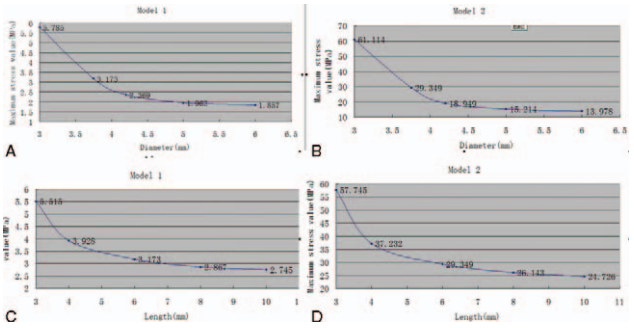

FIGURE 3. The influence of implant diameter and length on the orbital bone maximum stress values. (A) In model 1, the reductions of the maximum stress values were 45.2% (diameter of 3.0–3.75 mm), 25.3% (diameter of 3.75–4.2 mm), 17.2% (diameter of 4.2–5.0 mm), and 5.4% (diameter of 5.0–6.0 mm) respectively. (B) In model 2, the reductions of the maximum stress values in the bone around the orbital implant were 51.9% (diameter of 3.0–3.75 mm), 35.4% (diameter of 3.75–4.2 mm), 19.7% (diameter of 4.2–5.0 mm), and 8.1% (diameter of 5.0–6.0 mm) respectively. (C) In model 1, the reductions of the maximum stress values were 28.8% (length of 3–4 mm), 19.2% (length of 4–6 mm), 9.6% (length of 6–8 mm), and 4.3% (length of 8–10 mm), respectively. (D) In model 2, the reductions of the maximum stress values in the bone around the orbital implant were 35.5% (length of 3–4 mm), 21.1% (length of 4–6 mm), 10.9% (length of 6–8 mm), and 5.4% (length of 8–10 mm), respectively.

The relation between maximum stress values and implant length showed a similar trend as for the variable diameters (Fig. 3C and D). However, compared with the results for varying implant diameter, there was a smaller effect of implant length on stress in the orbital bone. In model 1, the maximum stress value in the bone around the orbital implant with a length of 4 mm was 28.8% smaller than the length of 3 mm implant. The reductions of the maximum stress values were 19.2% (length of 4–6 mm), 9.6% (length of 6–8 mm), and 4.3% (length of 8–10 mm) respectively. In model 2, the reductions of the maximum stress values in the bone around the orbital implant were 35.5% (length of 3–4 mm), 21.1% (length of 4–6 mm), 10.9% (length of 6–8 mm), and 5.4% (length of 8–10 mm) respectively.

DISCUSSION

Three-dimensional finite element analysis is a numerical stress analysis technique that is widely used to study engineering and biomechanical problems.[12] This technique has the following advantages: it is noninvasive; the amount of stress experienced at any given point can be theoretically measured; the material properties of craniofacial structures can be assigned to the nearest one that possibly can simulate this environment in vitro; the point of application, magnitude, and direction of a force may easily be varied to simulate a clinical situation; reproducibility does not affect the physical properties of the material involved; and the study can be repeated as many times as the operator wishes. The results of the finite element analysis computation depend on many individual factors, including material properties, boundary conditions, interface definition, and also on the overall approach to the model.

The orbital implant failure rate is high (between 35% and 75% after 3–14 years of follow-up). In general, bone sites in the orbital region are thin and irregular. They are often heavily compacted, with little or no marrow, and may lack the blood supply necessary to maintain an adequate bone–implant interface.[5–8] Therefore, it is the guarantee for long-term success rate of orbital implant to choose an appropriate orbital implant, provide a reasonable biomechanical environment for orbital implant osseointegration, and ensure stable bone–tissue interface around the implant. In which length and diameter of implant are very important factors.

At present, there are still no reports about 3D finite element mechanical analysis of orbital implant in craniofacial structures. Orbital implant material, surgical operation, and implant osseointegration are almost the same with dental implantation. As for the differences between these 2: the orbital implants have different length and diameter; the external loading of implants has different intensity and direction.

Literatures possess different viewpoints about the influence of diameter and length on stress distribution of bone around the dental implant. According to some researches, bone interface stress will be greatly affected by jaw height rather than the dental implant length.[13] There is no significant difference in the maximum stress

between the short implant and the long implant.[14] However, according to some other studies, the peak value of implantation torsion and bearing capacity for lateral force have obvious correlation with implant length and diameter.[15] Length and diameter of implant is closely related to long-term success rate of implant and short implant has a higher failure rate.[16] According to this study, with the increase of implant length and diameter, maximum stress value at 2 models reduces, but the decrease value has a difference among different implant lengths and diameters. When the implant length rises from 3 to 4 mm or diameter rises from 3 to 3.75 mm, the maximum stress value reduces obviously at 2 models; when the length increases from 6 to 8 mm and 10 mm or diameter increases from 4.2 to 5.0 mm and 6.0 mm, the maximum stress value does not decrease obviously. As for the reason, the increased length and diameter of implant are mostly located in cancellous bone and it does not bear much stress distribution; stress distribution of orbital implant is mainly in cortical bone.

This research result also shows that in selection of orbital implant, there is no need to deliberately increase the implant length and diameter. Meanwhile, it is feasible to apply short orbital implant, but implant of 3 mm possesses a high stress, so the orbital rim with thick compact bone (1, 4, and 5 o'clock positions for a left eye and 7, 8, and 11 o'clock positions for a right) should be selected according to the circumstances. The results of this simulation study have shown that orbital implant diameter was more important for improved stress distribution than length. These likely result from the fact that stress distribution inside the bony socket is uneven, the elements exposed to maximum stress are located around the neck,[17] and therefore, the wider area in the cervical portion of the implant may better dissipate the external forces.

In clinical operation, orbital implant is often inserted perpendicular to the orbital rim, the directions of multiple implants parallel are not necessary. The presented study shows that maximum stress was located around the root of the orbital implant when the loading along the long axis of the implant or between the neck and the first thread of the orbital implant when the loading along an angle of 45° with the long axis of the implant. This result indicated that the direction of orbital implant can be adjusted to reduce implants neck stress concentration, and gain a reasonable stress distribution. In this way, long-term success rate of the orbital implant should be improved.

According to this research result, there are significant differences in the maximum stress in orbital bone when the loading with different directions on the implants of the same length and diameter. This result shows that loading directions have obvious effect on stress distribution of the interface. Further study is required as for the specific influence of orbital implant loading directions on stress distribution.

Matsuura et al[18] reported on cadavers that at the sites corresponding to potential placement sites for implants as the fixation source for ocular epitheses, the mean length of bone was 7.8 mm and the mean width was 8.3 mm, allowing the insertion of orbital implants as described in this study.

Once orbital implants are successfully placed, 3 basic retentive systems can be used: the magnet and keeper, the ball and keeper, and the bar and clip. In clinical treatment, the magnetic retention system is more popular than the others, primarily because of the ease with which the patient can position a magnetically retained prosthesis and also because they offer better access for hygiene procedures. In this study, magnetic retention system was used. Further research to assess the behavior and stress distribution of 3 retention systems associated with implant for orbital prosthesis may be the subject of future research.

CONCLUSIONS

This finite elemental analysis of loading on orbital implant to craniofacial model should contribute to optimal orbital implant choice and placement to achieve better long-term success rate of the orbital implant. This finite element study showed that increased orbital implant diameter better decreased the stress around the implant. From a biomechanical perspective, the optimum choice was an orbital implant with no less than 4.2 mm diameter allowed by the anatomy. In this study, the effect of implant length was less notable.

REFERENCES

1. Parel SM, Brånemark P-I, Tjellstrom A, et al. Osseointegration in maxillofacial prosthetics. Part II: extraoral applications. *J Prosthet Dent* 1986;5:600–606
2. Tolman DE, Desjardins RP, Jackson IT, et al. Complex craniofacial reconstruction using an implant-supported prosthesis: case report with long-term follow-up. *Int J Oral Maxillofac Implants* 1997;2:243–251
3. Kovács AF. A follow-up study of orbital prostheses supported by dental implants. *J Oral Maxillofac Surg* 2000;1:19–23
4. Leonardi A, Buonaccorsi S, Pellacchia V, et al. Maxillofacial prosthetic rehabilitation using extraoral implants. *J Craniofac Surg* 2008;2:398–405
5. Abu-Serriah MM, McGowan DA, Moos KF, et al. Outcome of extra-oral craniofacial endosseous implants. *Br J Oral Maxillofac Surg* 2001;4:269–275
6. Nishimura RD, Roumanas E, Moy PK, et al. Osseointegrated implants and orbital defects: U.C.L.A. experience. *J Prosthet Dent* 1998;3:304–309
7. Toljanic JA, Eckert SE, Roumanas E, et al. Osseointegrated craniofacial implants in the rehabilitation of orbital defects: an update of a retrospective experience in the United States. *J Prosthet Dent* 2005;2:177–182
8. Roumanas ED, Freymiller EG, Chang TL, et al. Implant-retained prostheses for facial defects: an up to 14-year follow-up report on the survival rates of implants at UCLA. *Int J Prosthodont* 2002;4:325–332
9. Zhang X, Chen S, Huang Y, et al. Computer-assisted design of orbital implants. *Int J Oral Maxillofac Implants* 2007;22:132–137
10. Zhang X, Chen SL, Zhang JM, et al. Fabrication of a surgical template for orbital implant placement: a case report. *Int J Oral Maxillofac Implants* 2010;25:826–830
11. Cattaneo PM, Dalstra M, Frich LH. A three-dimensional finite element model from computed tomography data: a semiautomated method. *Proc Inst Mech Eng* 2001;215:203–213
12. Korioth TW, Versluis A. Modeling the mechanical behavior of the jaws and their related structures by finite element (FE) analysis. *Crit Rev Oral Biol Med* 1997;8:90–104
13. Meijer HJ, Starman FJ, Boman F, et al. Stress distribution around dental implants: influence of superstructure, length of implants, and height of mandible. *J Prosthet Dent* 1992;68:96–100
14. Holmgren EP, Seckinger RJ, Kilgren LM, et al. Evaluating Parameters of osseointegrated dental implants using finite element analysis a two-dimensional comparative study examining the effects of implant diameter, implant shape, and load direction. *J Oral Implantol* 1998;24:80–88
15. Lim SA, Cha JY, Hwang CJ. Insertion torque of orthodontic miniscrews according to changes in shape, diameter and length. *Angle Orthod* 2008;78:234–240
16. Goodacre CJ, Kan JY, Rungcharassaeng K, et al. Clinical complications of osseointegrated implants. *J Prosthet Dent* 1999; 81:537–552
17. Meijer HJ, Starmans FJ, Steen WH, et al. Loading conditions of endosseous implants in an edentulous human mandible: a three-dimensional, finite-element study. *J Oral Rehabil* 1996;23: 757–763
18. Matsuura M1, Ohno K, Michi K, et al. Clinicoanatomic study on the craniofacial bones used for cranio- and maxillofacial implants. *Int J Oral Maxillofac Implants* 2002;17:121–129